PROCEEDINGS OF SCIENCE

Excited states and precision results for nucleon charges and form factors

Rajan Gupta,[a,*] **Tanmoy Bhattacharya,**[a] **Vincenzo Cirigliano,**[a] **Martin Hoferichter,**[b] **Yong-Chull Jang,**[c] **Balint Joo,**[d] **Emanuele Mereghetti,**[a] **Santanu Mondal,**[a,e] **Sungwoo Park,**[a,g] **Frank Winter**[g] **and Boram Yoon**[h]

[a] *Los Alamos National Laboratory, Theoretical Division T-2, Los Alamos, NM 87545, USA*

[b] *Albert Einstein Center for Fundamental Physics, Institute for Theoretical Physics, University of Bern, Sidlerstrasse 5, 3012 Bern, Switzerland*

[c] *Physics Department, Columbia University, New York, NY 10027, USA*

[d] *Oak Ridge Leadership Computing Facility, Oak Ridge National Laboratory, Oak Ridge, TN 37831, USA*

[e] *Department of Physics and Astronomy, Michigan State University, MI, 48824, USA*

[f] *Department of Computational Mathematics, Science and Engineering, Michigan State University, MI, 48824, USA*

[g] *Jefferson Lab, 12000 Jefferson Avenue, Newport News, Virginia 23606, USA*

[h] *Los Alamos National Laboratory, Computer Computational and Statistical Sciences Division, CCS-7, Los Alamos, NM 87545, USA*

E-mail: rajan@lanl.gov

The exponentially falling signal-to-noise ratio in all nucleon correlation functions, and the presence of towers of multihadron excited states with relatively small mass gaps makes extraction of matrix elements of various operators within the ground state nucleon challenging. Theoretically, the allowed positive parity states with the smallest mass gaps are the $N(\boldsymbol{p})\pi(-\boldsymbol{p})$, $N(\boldsymbol{0})\pi(\boldsymbol{0})\pi(\boldsymbol{0})$, $N(\boldsymbol{p})\pi(\boldsymbol{0})$, $N(\boldsymbol{0})\pi(\boldsymbol{p})$, ..., states. A priori, the contribution of these states arises at one loop in chiral perturbation theory (χPT), however, in many cases the contributions are enhanced. In this talk, I will review four such cases: the correlation functions from which the axial form factors, electric and magnetic form factors, the Θ-term contribution to neutron electric dipole moment (nEDM), and the pion-nucleon sigma term are extracted. Including appropriate multihadron states in the analysis can lead to significantly different results compared to standard analyses with the mass gaps taken from fits to 2-point functions. The χPT case for $N\pi$ states is the most clear in the axial/pseudoscalar form factors which need to satisfy the PCAC relation between them. Our analyses, supported by χPT, suggests similarly large effects in the calculations of the Θ-term and the pion-nucleon sigma term that have significant phenomenological implications.

The 38th International Symposium on Lattice Field Theory, LATTICE2021 26th-30th July, 2021 Zoom/Gather@Massachusetts Institute of Technology

*Speaker

PoS(LATTICE2021)478

1. Introduction

Precision calculations of the matrix elements of various local and nonlocal operators composed of quark and gluon fields provide detailed knowledge of the hadron structure. Simulations are being done with realistic values of the light (mostly assuming isospin symmetry, $m_u = m_d$), strange and charm quark masses over a range of lattice spacings $0.04 \lesssim a \lesssim 0.15$ fm that provide good control over discretization errors [1–3]. Finite volume corrections in nucleon properties are observed to be small for $M_\pi L \geq 4$ [1–3]. The main challenges to obtaining percent level results are statistical errors, excited-states contributions (ESC), and the concomitant unresolved chiral behavior. With $O(10^6)$ measurements on about 5000 configurations, one can get a good statistical signal up to ≈ 2 fm in 2-point correlation functions and up to ≈ 1.5 fm in 3-point functions [2]. Even at these source-sink separations, ESC are found to be large. To remove these contributions using fits to the spectral decomposition of these correlation functions requires knowing the energies of the excited states that make significant contributions. Possible states include radial excitations and towers of multihadron states, $N(\boldsymbol{p})\pi(-\boldsymbol{p})$, $N\pi\pi$, ..., characterized by relative momenta $\boldsymbol{p}$ and having the quantum numbers of the nucleon. This talk discusses three quantities whose values extracted using the standard analysis (using the spectrum obtained from fits to the 2-point functions) that misses the $N\pi$ states differs very significantly from those obtained including the lowest allowed $N\pi$, $N\pi\pi$ states that are motivated by chiral perturbation theory (χPT). Resolving all the excited states that contribute significantly to a given correlation function is, therefore, essential to progress.

2. Spectrum from nucleon 2-point function

The spectrum in a finite box of a nucleon with momentum $\boldsymbol{p} = \mathbf{n}2\pi/La$ can be determined from fits to the spectral decomposition of the two-point function $C^{\rm 2pt}$:

$$C^{\rm 2pt}(\tau;\boldsymbol{p}) = \sum_i |\mathcal{A}_i(\boldsymbol{p})|^2 e^{-E_i(\boldsymbol{p})\tau} \,. \tag{1}$$

Here E_i are the energies and $\mathcal{A}_i$ are the corresponding amplitudes for the creation/annihilation of a given state $|i\rangle$. In all the calculations discussed here, $\mathcal{N}(x) = \epsilon^{abc}\left[q_1^{aT}(x)C\gamma_5\frac{(1\pm\gamma_4)}{2}q_2^b(x)\right]q_1^c(x)$ was used for the interpolating operator at both the source and the sink. In this setup, states with small $\mathcal{A}_i$ will be missed in the fit to Eq. (1) and thus in the standard analysis of 3-point functions.

An example of the conumdrum of ESC is shown in Fig. 1 using high statistics data and fit to Eq. (1) truncated at four states. (See Ref. [2] for details.) The left panel shows the standard analysis with wide priors used only to stabilize the fit, while the right panel shows a fit with a narrow prior for E_1 taken to be the energy of a non-interacting $N(\mathbf{1})\pi(-\mathbf{1})$ state. The resulting E_1 are about 1.5 and 1.2 GeV, respectively. The two outcomes are not distinguished by the augmented χ^2 minimized in the fits. In fact, in 4-state fits there is a whole region of parameter space that gives similar χ^2 in which $1.2 < E_1 < 1.5$ GeV is equally likely. Furthermore, assuming $R_1 \equiv |\mathcal{A}_1/\mathcal{A}_0|^2 = 1$, the contribution of a state with $\Delta E_1 = 300$ MeV is still 20% (5%) at $\tau/a = 11$ (22), i.e., at source-sink separation τ of 1fm (2fm). Thus, very high precision data at $\tau/a > 1$ fm are needed to resolve ES.

Bottom line: methods to beat the exponential, $e^{-(M_N - 1.5M_\pi)\tau}$, decay in signal in all nucleon correlation functions are needed. Recognizing that the excited state spectrum is not easy to

resolve from fits to Eq. (1) with data generated using a single interpolating operator $\mathcal{N}$, developing the computationally challenging technology for using a variational basis of operators including multihadron states such as $N\pi$, $N\pi\pi$ is essential. Motivation for including $N\pi$, $N\pi\pi$, ... states in the analysis of 3-point functions comes from theory (χPT), and in the case of the axial form factors from satisfying the PCAC relation as discussed next. Throughout this talk, "standard" analysis will imply using the spectrum from fits to the 2-point correlator ($E_1 \geq N(1440)$), whereas "$N\pi$" analysis implies that E_1 used is essentially the non-interacting energy of the $N\pi$ state calculated on that ensemble.

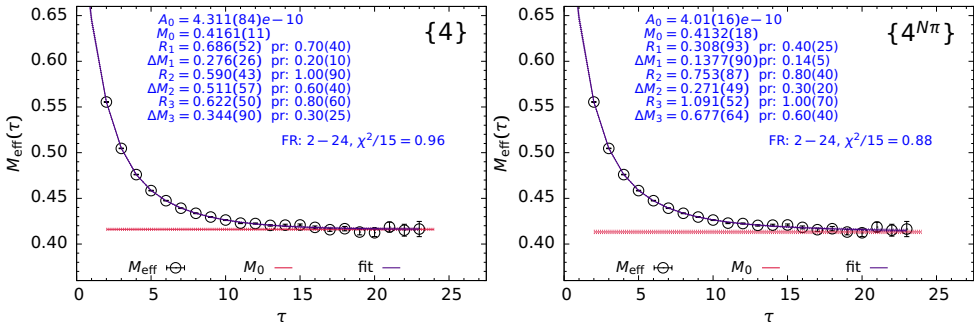

Figure 1: Nucleon effective mass plot using data from $64^3 \times 128$ lattices at $a = 0.091$ fm and $M_\pi = 170$ MeV. The statistical sample consists of 3000 configurations with 320 measurements on each configuration. Errors on the data are calculated using a single elimination jackknife procedure on data binned over 6 configurations.

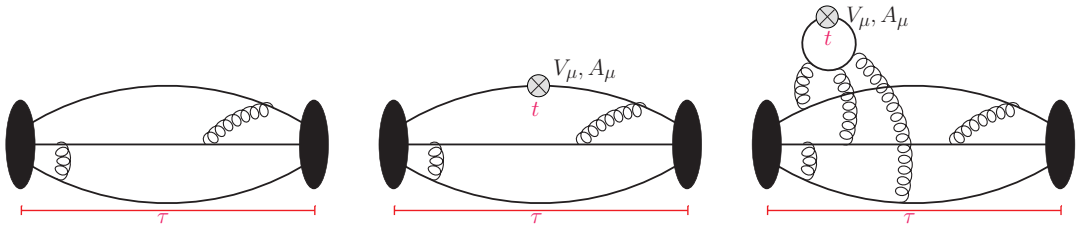

Figure 2: Quark line diagrams illustrating the 2-point (left), 3-point connected (middle) and 3-point disconnected (right) correlation functions with the insertion of the vector V_μ or the axial A_μ currents.

3. Excited states in 3-point functions

The spectral decomposition of any three-point function $C_O^{\rm 3pt}$ (see Fig. 2 for illustration) is:

$$C_O^{\rm 3pt}(\tau;t) = \sum_{i,j} \mathcal{A}_i \mathcal{A}_j^{-\boldsymbol{q}} \langle i|O_{\boldsymbol{p}}|j^{-\boldsymbol{q}}\rangle e^{-E_j t - E_i(\tau - t)} \,. \tag{2}$$

The operator inserts momentum $\boldsymbol{q}$, $\mathcal{N}$ at the sink is projected to $\boldsymbol{p} = 0$, making the nucleon momentum $\boldsymbol{p} = -\boldsymbol{q}$ at the source. The spin projection operator used for the forward propagating nucleon is $(1+\gamma_4)(1+i\gamma_5\gamma_3)/2$. It is important to note that for $\boldsymbol{q} \neq 0$ case relevant to form factors, the allowed excited states on the two sides of the operator are different: for example they can be $N(\boldsymbol{k})\pi(-\boldsymbol{k}), \forall \boldsymbol{k} \neq 0$ on the $\boldsymbol{p} = 0$ side and $N(\boldsymbol{k})\pi(-(\boldsymbol{p}+\boldsymbol{k}))$ or $N(-(\boldsymbol{p}+\boldsymbol{k})\pi(\boldsymbol{k}), \forall \boldsymbol{k}$ on the $\boldsymbol{p} \neq 0$ side. Thus different towers of multihadron, in addition to single-particle, excited states contribute.

At 1-loop in χPT, there is a long distance pion loop in all possible configurations [5] which can, a priori, give a large correction to any 3-point function. The question is whether this or higher

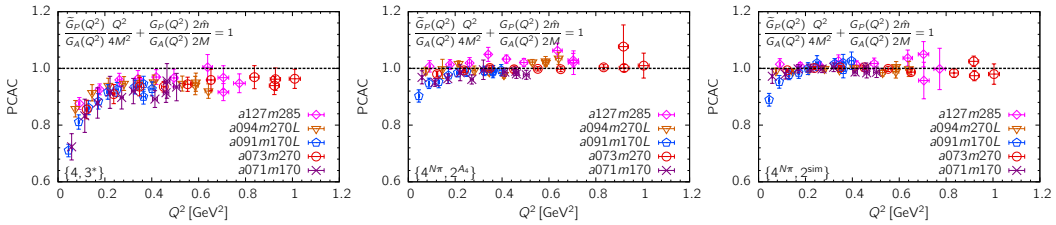

Figure 3: The three panels show the degree to which the axial form factors satisfy the PCAC relation, Eq. (4), for three analysis strategies specified at the bottom left corner and described in the text. Data from Ref. [2].

order contributions are significant? We discuss three cases where these ESC are, in fact, enhanced, and one case (EM form factors) where they are not.

4. Axial vector form factors

The axial and pseudoscalar form factors, $G_A(q^2)$, $\widetilde{G}_P(q^2)$ and $G_P(q^2)$ are obtained by decomposing the following matrix elements (ME) calculated within the nucleon ground state $|N(\boldsymbol{p}_i, s_i)\rangle$:

$$\begin{aligned}\left\langle N(\boldsymbol{p}_f, s_f)|A_\mu(\boldsymbol{q})|N(\boldsymbol{p}_i, s_i)\right\rangle &= \overline{u}_N(\boldsymbol{p}_f, s_f)\left(G_A(q^2)\gamma_\mu + q_\mu \frac{\widetilde{G}_P(q^2)}{2M_N}\right)\gamma_5 u_N(\boldsymbol{p}_i, s_i),\\ \left\langle N(\boldsymbol{p}_f)|P(\boldsymbol{q})|N(\boldsymbol{p}_i)\right\rangle &= \overline{u}_N(\boldsymbol{p}_f) G_P(q^2)\gamma_5 u_N(\boldsymbol{p}_i),\end{aligned} \tag{3}$$

where $A_\mu = Z_A \overline{u}\gamma_\mu\gamma_5 d$ and $P = Z_P \overline{u}\gamma_5 d$ are the renormalized isovector axial and pseudoscalar currents. These three form factors have to satisfy, up to discretization errors, the following PCAC relation, a consequence of the axial Ward identity, $\partial_\mu A_\mu - 2Z_m m P = 0$:

$$2\widehat{m} G_P(Q^2) = 2M_N G_A(Q^2) - \frac{Q^2}{2M_N}\widetilde{G}_P(Q^2), \tag{4}$$

where $\widehat{m} \equiv Z_m Z_P (m_u + m_d)/(2Z_A)$ is the average bare PCAC mass of the u and d quarks. Figure 3, taken from Ref. [2], shows the degree to which the axial form factors satisfy Eq. (4), with ME obtained from 3 analysis strategies: $\{4, 3^*\}$—standard analysis with a 3-state fit to the A_i and P 3-point correlators; $\{4^{N\pi}, 2^{A_4}\}$—a 2-state fit to the A_i and P 3-point correlators with E_1 determined from a fit to the A_4 correlator; and $\{4^{N\pi}, 2^{\rm sim}\}$—a simultaneous 2-state fit to all five A_μ and P 3-point correlators with E_1 left as a free parameter. The data show that the standard analysis, $\{4, 3^*\}$, fails by about 50% at $M_\pi = 135$ MeV [4]. Including the $N\pi$ state, ($\{4^{N\pi}, 2^{A_4}\}$ and $\{4^{N\pi}, 2^{\rm sim}\}$ strategies), significantly improves the agreement with PCAC, with the remaining difference attributable to possible discretization errors and/or contributions of additional excited states. The increase in deviation (and difference from "$N\pi$") as $Q^2 \to 0$ and $M_\pi \to 135$ MeV is correlated with the growth in the difference in E_1 between the "standard" and "$N\pi$" analyses. χPT analysis cements this understanding of enhancement [5]–the axial current couples to a light pion, and this interaction vertex can be anywhere in the spatial 3-volume: a well-known observation enshrined in the pion-pole dominance hypothesis. This volume enhancement causes a large $N\pi$ contribution. Thus the case for including the $N\pi$ state in analysis of the axial FF is clear. The question therefore is–what ES make significant contributions in a given $C_O^{\rm 3pt}(\tau; t)$, and including them.

Knowing that "$N\pi$" states contribute to axial/pseudoscalar FF, the precision of calculations of the axial charge g_A [1, 3] is also in question. Again the issue is the size of the integrated contribution from the tower of $N(\boldsymbol{k})\pi(-\boldsymbol{k})$ excited states. One way forward, advocated in [2], is to demonstrate the necessary consistency check–the value of g_A in the continuum limit from the forward matrix element has to agree with that obtained by extrapolating the axial form factor $G_A(Q^2)$ to $Q^2 = 0$. This, of course, requires controlling all the systematics in both calculations.

5. Electric and magnetic form factors

The Sachs electric, $G_E(Q^2)$, and magnetic, $G_M(Q^2)$, form-factors have been measured extensively in electron-nucleon scattering experiments. For the current status of the possible resolution of the discrepancy in the proton charge radius between the electron scattering and muon capture experiments see Ref. [6]. Compared to lattice calculations, the experimental data for the form factors is very precise and, therefore, they provide a test for the lattice methodology.

Chiral PT analysis by Bär in Ref. [7] indicates a $\approx 5\%$ effect due to the pion loop. The Q^2 dependence and the magnitude of the effect is consistent with the pattern seen in a summary of world lattice data shown in fig. [22] in Ref. [8]. In this case, one expects contributions from vector current coupling to rho to two pions (vector meson dominance), however, since the ρ-meson is heavy, the enhanced coupling of the vector current to the ρ-meson may be negated by its heavier mass.

Figure 4 shows our latest data from 2 + 1-flavor clover simulations [2] plotted versus Q^2/M_N^2. We find a much better agreement with the Kelly parameterization over the whole range $0.04 < Q^2 < 1.2$ GeV^2 compared to previous lattice data [8]. The differences in form factors between analyses without (left panel) and with (middle panel) a low-mass excited state ($N\pi$ or $N\pi\pi$) or with the mass gap determined from the 3-point functions themselves (right panel) are small. Furthermore, we observe insensitivity of the data to lattice spacing a and the pion mass. We are testing this favorable situation, ie, EM form factors showing small systematics, by increasing the statistics and adding more ensembles. Once validated, lattice QCD is poised to provide precision results in the near future.

6. Contribution of the Θ-term to neutron EDM

The Θ-term $\left(\Theta\frac{iG^a_{\mu\nu}\widetilde{G}^a_{\mu\nu}}{32\pi^2}\right)$ is a P and T violating dimension four operator (also $\not{C}\not{P}$ if CPT is conserved) allowed in the standard model. It contributes an amount $d_n = X\overline{\Theta}$ to the neutron electric dipole moment (nEDM). Here $\overline{\Theta}$ is the convention independent coupling and $X \equiv \lim_{q^2\to 0}\frac{F_3(q^2)}{2M_N\overline{\Theta}}$ is given by the $\not{C}\not{P}$ part of the electromagnetic form factor F_3 calculated using lattice QCD [9]. Using the current upper bound on the nEDM, $|d_n| < 1.8\times 10^{-26}$ e cm (90% CL) [10], on gets $\overline{\Theta} < 10^{-10}$, an unnaturally small number. Since each $\not{C}\not{P}$ interaction contributes to the nEDM, a value or bound on d_n constraints the parameter space of possible $\not{C}\not{P}$ couplings. Our goal is to determine the ME that connect d_n to the couplings, i.e., the analogue of X from F_3 in the Θ-term example, for the Weinberg, quark chromo EDM and 4-fermion low-energy effective operators up to mass dimension 6 that encapsulate $\not{C}\not{P}$ in the quark-gluon sector [11] (see talk by T. Bhattacharya, *ibid*).

A χPT analysis in [9] showed that the gap between the ground and excited states contributing to the CP-odd components of the three-point function with the insertion of the $\bar{\Theta}$-term is of the order of the pion mass M_π. Again, this can be intuitively understood as coming from a long-range pion loop

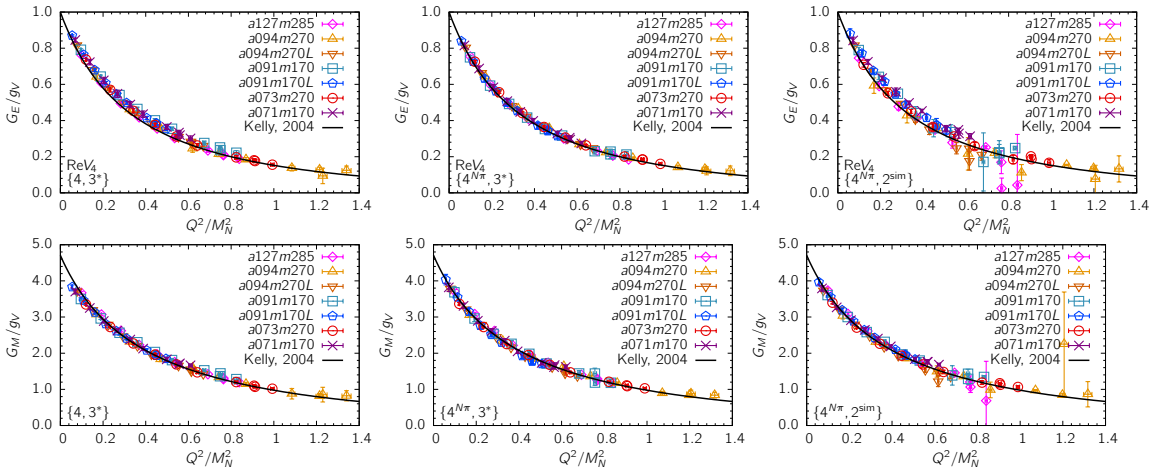

Figure 4: $G_E(Q^2)$ and $G_M(Q^2)$ plotted versus Q^2/M_N^2. Comparison of data extracted using 3 strategies for controlling ESC: left labeled $\{4, 3^*\}$ is the standard 3-state analysis; middle labeled $\{4^{N\pi}, 3^*\}$ inputs a narrow prior for E_1 corresponding to a $N\pi\pi$ state in a 3-state fit; and right labeled $\{4^{N\pi}, 2^{\rm sim}\}$ is a simultaneous 2-state fit to all V_μ channels with E_1 left a free parameter. See Ref. [2] for details.

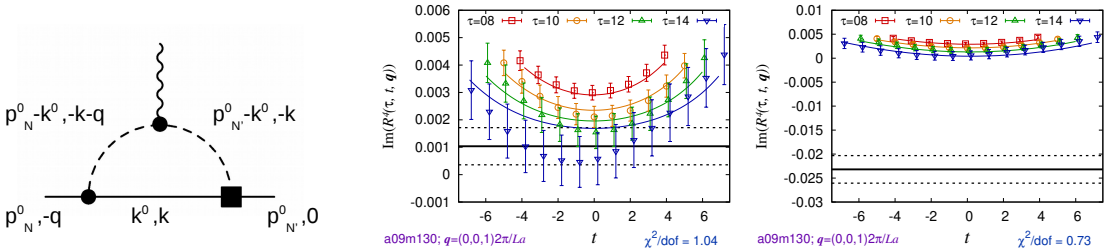

Figure 5: (Left) Leading order diagram for the excited states contribution to the three-point function C^{μ}_{3pt} in chiral perturbation theory. A black square denotes an insertion of the CP-odd pion-nucleon couplings $\bar{g}_0$. Filled circles denote CP-even pion-nucleon and pion-photon couplings. A ground state estimate from a two-state fit with E_1 taken from the standard three-state fit to the two-point function (left panel) is compared to that with E_1 set equal to the non-interacting energy of the $N\pi$ state (right panel). The data are from a $a \approx 0.09$ fm, $M_\pi = 135$ MeV ensemble. The χ^2/dof of the two sets of fits are comparable, but the extrapolated ground state value (solid black line) is vastly different. All three panels are reproduced from [9].

[12] (Fig. 5 left). In Fig. 5 we also show an example of the big difference in results (solid black lines) for the ground state matrix elements extracted from a standard analysis, a three-state fit with E_1 from the two-point function, (middle panel) versus using the non-interacting energy of the $N\pi$ state (right panel). The resulting values of d_n are very different and results including $N\pi$ states are much larger! Our work [9] made 2 points: (i) the errors in all existing lattice calculations of the contribution of the Θ–term to nEDM are too large to quote a reliable value, and (ii) resolving the excited state spectrum is essential for precision determination of X; if $N\pi$ states do give dominant contamination, then d_n will be larger and calculable sooner! An exception to the poor signal in nEDM derived from calculations of the F_3 form factor (Θ, Weinberg, quark chromo; 3 of 5 effective $D \le 6$ $\not{C}\not{P}$ operators arising from BSM) is the (fourth) quark EDM operator that has been determined with $\lesssim 5\%$ uncertainty [13, 14]. For it, $X = g_T^{u,d,s,c,b}$. These tensor charges have small ESC and are insensitive to the details of the excited-state spectrum used, ie, whether $N\pi$ states are included in the fits to remove ESC [1, 3, 13].

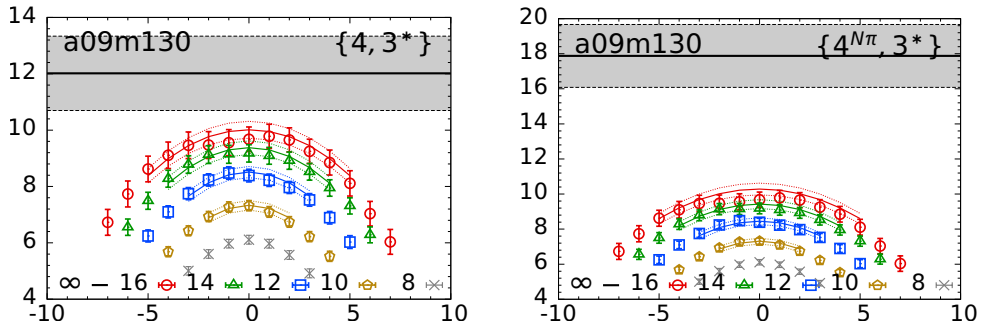

Figure 6: The data for g_S^{u+d+2l} from the physical mass, $a09m130$ ensemble and the two fits to remove ESC. (Left) standard analysis and (Right) including $N\pi$ and $N\pi\pi$ states. Both panels are reproduced from [14].

7. The pion-nucleon sigma term

The pion–nucleon σ-term is $\sigma_{\pi N} \equiv m_{ud}\, g_S^{u+d} \equiv m_{ud}\, \langle N(\mathbf{k}, s)|\bar{u}u + \bar{d}d|N(\mathbf{k}, s)\rangle$. The scalar charge g_S^q is the forward matrix element of the scalar density $\bar{q}q$ between the nucleon ground state,

$$g_S^q = \langle N(\mathbf{k} = 0, s)|\bar{q}q|N(\mathbf{k} = 0, s)\rangle. \tag{5}$$

The $\sigma_{\pi N}$ is a fundamental parameter of QCD–it quantifies the amount of the nucleon mass that comes from u- and d-quark masses being non-zero. Also, the scalar charge g_S enters into the spin independent cross-section of dark matter with nuclear targets [15, 16], lepton flavor violation in $\mu \longrightarrow e$ conversion in nuclei [17, 18], and in electric dipole moments [19, 20]. Thus knowing $\sigma_{\pi N}$ and g_S^q accurately is important. In addition to lattice calculations, $\sigma_{\pi N}$ has also been extracted phenomenologically from $\pi - N$ scattering via the Cheng–Dashen low-energy theorem [21, 22].

The current status of lattice calculations of $\sigma_{\pi N}$ and comparison to phenomenology has been reviewed by FLAG [1, 3]. The reviewed results show a tension between the lattice estimates that favor $\sigma_{\pi N} \approx 40$ MeV versus values from phenomenology centered around $\sigma_{\pi N} \approx 60$ MeV [23, 24].

Our recent lattice calculation [14] has been performed in the isospin symmetric limit, i.e., with $m_{ud} = (m_u + m_d)/2$ the average of the light quark masses. The N^{2}LO χPT analysis showed that there is an enhanced contribution from $N\pi$ and $N\pi\pi$ states due to the large coupling of the scalar source to two pions, i.e., a large quark condensate. Our result with the standard analysis is $\sigma_{\pi N} \approx 40$ MeV (consistent with previous lattice estimates) while the one including contributions of $N\pi$ and $N\pi\pi$ states gave $\sigma_{\pi N} \approx 60$ MeV, which is consistent with phenomenology. The data from the physical mass, $a09m130$, ensemble and the two fits to remove ESC are shown in Fig. 6. Again, the two fits with very different results are not differentiated by the χ^2. To reach discrimination will, we estimate, require similar precision data at $\tau = 18$ and 20, i.e., a $\geq$10X increase in statistics.

8. Conclusions

The lattice methodology for the calculations of nucleon matrix elements and their extraction from correlation functions using spectral decomposition is robust, however, the two related issues of the exponential decay of the statistical signal with source-sink separation in all nucleon n-point functions and the contribution of low-lying multihadron excited states have to be addressed

before precision results can be obtained. Here, we review three examples, (i) the axial form factors $G_A(q^2)$, $\widetilde{G}_P(q^2)$ and $G_P(q^2)$; (ii) the Θ-term contribution to nEDM; and (iii) the pion-nucleon sigma term, for which χPT indicates a large contribution and including "$N\pi$" changes the results very significantly. The case for including $N\pi$ states in the analysis of axial form factors is strengthened by (i) the strong χ^2 preference in fits to the 3-point function with the insertion of the A_4 operator and (ii) the resulting form factors satisfy the PCAC relation to within expected discretization errors. Unfortunately, for all other quantities, fits to the current lattice data do not distinguish between the "standard" and "$N\pi$" analyses on the basis of χ^2. (The weakness in the "$N\pi$" analysis for most quantities is the narrow priors used for excited state energies.) Thus, we resort to χPT for guidance on which analysis to choose. In future, with increased statistics, we anticipate fits can be made directly to 3-point functions with one or even two excited states and their energies E_i left as free parameters.

Another point in support of taking input from χPT in the ESC fits is that results of the same analysis are used for making the chiral fits to quantify the behavior versus M_π^2 and get the final results at the physical pion mass and in the continuum limit. For self consistency, one should include the states that make a significant contribution in both parts of the analysis.

Promising future approaches include (i) to overcome the signal to noise problem develop methods based on analytic continuation of the contour of integration (see Refs. [25, 26]), and (ii) to use a variational basis of nucleon interpolating operators that includes multihadron operators to project on to the ground state of the nucleon at much earlier source-sink separations. Hopefully, one or more of such novel methods will, in the near future, break the logjam.

Acknowledgments

The calculations presented are based on two sets of ensembles: the 2 + 1 + 1-flavor HISQ ensembles generated by the MILC collaboration and the 2 + 1-flavor Wilson-clover ensembles generated by the JLAB/W&M/LANL/MIT collaborations. The calculations used the Chroma software suite [27]. We gratefully acknowledge computing resources provided by NERSC, OLCF at Oak Ridge, USQCD and LANL Institutional Computing. Support for this work was provided the U.S. DOE Office of Science HEP and NP, the SNSF, and by the LANL LDRD program.

References

[1] Flavour Lattice Averaging Group collaboration, S. Aoki, Y. Aoki, D. Bečirević, T. Blum, G. Colangelo, S. Collins et al., *Eur. Phys. J. C* **80** (2020) 113 [1902.08191].

[2] S. Park, R. Gupta, B. Yoon, S. Mondal, T. Bhattacharya, Y.-C. Jang et al., 2103.05599.

[3] Y. Aoki et al., 2111.09849.

[4] Y.-C. Jang, R. Gupta, B. Yoon and T. Bhattacharya, *Phys. Rev. Lett.* **124** (2020) 072002 [1905.06470].

[5] O. Bär, *Phys. Rev. D* **99** (2019) 054506 [1812.09191].

[6] W. Xiong et al., *Nature* **575** (2019) 147.

[7] O. Bär and H. Čolić, *Phys. Rev. D* **103** (2021) 114514 [2104.00329].

[8] Y.-C. Jang, R. Gupta, H.-W. Lin, B. Yoon and T. Bhattacharya, *Phys. Rev. D* **101** (2020) 014507 [1906.07217].

[9] T. Bhattacharya, V. Cirigliano, R. Gupta, E. Mereghetti and B. Yoon, *Phys. Rev. D* **103** (2021) 114507 [2101.07230].

[10] nEDM collaboration, C. Abel et al., *Phys. Rev. Lett.* **124** (2020) 081803 [2001.11966].

[11] M. Pospelov and A. Ritz, *Annals Phys.* **318** (2005) 119 [hep-ph/0504231].

[12] R. J. Crewther, P. Di Vecchia, G. Veneziano and E. Witten, *Phys. Lett. B* **88** (1979) 123.

[13] T. Bhattacharya, V. Cirigliano, R. Gupta, H.-W. Lin and B. Yoon, *Phys. Rev. Lett.* **115** (2015) 212002 [1506.04196].

[14] R. Gupta, S. Park, M. Hoferichter, E. Mereghetti, B. Yoon and T. Bhattacharya, *Phys. Rev. Lett.* **127** (2021) 242002 [2105.12095].

[15] A. Bottino, F. Donato, N. Fornengo and S. Scopel, *Astropart. Phys.* **18** (2002) 205 [hep-ph/0111229].

[16] M. Hoferichter, P. Klos, J. Menéndez and A. Schwenk, *Phys. Rev. Lett.* **119** (2017) 181803 [1708.02245].

[17] V. Cirigliano, R. Kitano, Y. Okada and P. Tuzon, *Phys. Rev. D* **80** (2009) 013002 [0904.0957].

[18] A. Crivellin, M. Hoferichter and M. Procura, *Phys. Rev. D* **89** (2014) 093024 [1404.7134].

[19] J. Engel, M. J. Ramsey-Musolf and U. van Kolck, *Prog. Part. Nucl. Phys.* **71** (2013) 21.

[20] J. de Vries, E. Mereghetti, C.-Y. Seng and A. Walker-Loud, *Phys. Lett. B* **766** (2017) 254 [1612.01567].

[21] T. P. Cheng and R. F. Dashen, *Phys. Rev. Lett.* **26** (1971) 594.

[22] L. S. Brown, W. J. Pardee and R. D. Peccei, *Phys. Rev. D* **4** (1971) 2801.

[23] M. Hoferichter, J. Ruiz de Elvira, B. Kubis and Ulf-G. Meißner, *Phys. Rev. Lett.* **115** (2015) 092301 [1506.04142].

[24] J. Ruiz de Elvira, M. Hoferichter, B. Kubis and Ulf-G. Meißner, *J. Phys. G* **45** (2018) 024001 [1706.01465].

[25] M. L. Wagman and M. J. Savage, *Phys. Rev. D* **96** (2017) 114508 [1611.07643].

[26] W. Detmold, G. Kanwar, H. Lamm, M. L. Wagman and N. C. Warrington, *Phys. Rev. D* **103** (2021) 094517 [2101.12668].

[27] SciDAC, LHPC, UKQCD collaboration, R. G. Edwards and B. Joó, *Nucl. Phys. Proc. Suppl.* **140** (2005) 832 [hep-lat/0409003].